



Differential Presentation of a Single Antimicrobial Peptide is Sufficient to Identify LPS from Distinct Bacterial Samples

Journal:	<i>Analyst</i>
Manuscript ID	AN-ART-09-2019-001781.R1
Article Type:	Paper
Date Submitted by the Author:	08-Oct-2019
Complete List of Authors:	Reichart, Timothy; Ecole Polytechnique Federale de Lausanne, Swiss Institute of Life Sciences; Combat Capabilities Development Command Soldier Center, Office of the Chief Scientist Uzarski, Joshua; Combat Capabilities Development Command, CB Innovative Material and Ensemble Development Team Mello, Charlene; Combat Capabilities Development Command Soldier Center, Office of the Chief Scientist

Differential Presentation of a Single Antimicrobial Peptide is Sufficient to Identify LPS from Distinct Bacterial Samples

Timothy M. Reichart^{1,3}, Joshua R. Uzarski², and Charlene M. Mello¹

¹Office of the Chief Scientist, Combat Capabilities Development Command Soldier Center, Natick, MA 01760, United States

²CB Innovative Material and Ensemble Development Team, Combat Capabilities Development Command, Natick, MA 01760, United States

³Present address: Swiss Institute for Experimental Cancer Research, School of Life Sciences. Ecole Polytechnique Fédérale de Lausanne, 1015 Lausanne, Switzerland

ABSTRACT: Rapid detection and identification of bacteria is important for human health, biodefense, and food safety. Small arrays of different antimicrobial peptides (AMPs) enable identification of lipopolysaccharide (LPS) samples from a variety of bacterial species and strains. A model system for examining how peptide presentation effects LPS detection is the sheep myeloid antimicrobial peptide (SMAP-29), which contains a helix-turn-helix motif. Varying the cysteine attachment site on SMAP-29 controls the three-dimensional presentation of the peptide on the surface, altering the ability of the peptide to discriminate between LPS samples. A small array of only SMAP-29 variants—and no other peptides—is capable of discriminating among LPS samples from multiple bacterial species, as well as between different strains within the same species, with high accuracy.

INTRODUCTION

Detection of pathogenic bacteria is critically important to global health.¹ Bacterial infections are the leading cause of death in developing nations, and antibiotic-resistant bacteria are a continually growing threat. The tremendous power of antibiotics has led to their widespread overuse, which only furthers the growing crisis in antibiotic resistance. Reliable, fast, and inexpensive diagnostic techniques could help ensure appropriate and effective antibiotic use.

The principal component of the outer leaflet of Gram-negative bacterial membranes is lipopolysaccharide (LPS), and, as befits its other name of endotoxin, is often highly toxic to mammalian cells. In bacterial infection, recognition of LPS by the immune system causes a major release of inflammatory cytokines which can result in major organ failure and death.² Exposure to LPS in bacterial infection results in approximately 200,000 deaths per year due to septic shock in the United States alone.³ LPS in the bloodstream has also been linked to sudden infant death syndrome (SIDS) and severe nerve damage.⁴ Detection of LPS is plainly important in infection, but also has important applications outside of the clinic. *Salmonella enterica* is responsible for up to 1.4 million illnesses in the United States every year.⁵ It is notorious for contaminating the food supply, particularly raw meats, eggs, vegetables, fruits, and even rice and wheat cereals. LPS in water supplies can pose a severe threat to immunocompromised individuals, particularly in the developing world or when there are failures in developed water systems.⁶ LPS-contaminated devices can cause severe challenges to users of medical devices and injectables.⁷

There are a number of creative methods currently in use to test for the presence of LPS. The rabbit pyrogen test involves injecting test material into a rabbit's bloodstream and monitoring the animal for increases in temperature.⁸ The monocyte activation test (MAT) avoids the use of animals by using the production of cytokines from monocytes.⁹ Both these pyrogen techniques detect LPS, but also respond to a range of non-endotoxin pyrogens. The discovery in 1956 that the blood of horseshoe crabs coagulates upon exposure to Gram-negative bacteria led to the development of the limulus amoebocyte lysate (LAL) test, which amplifies the detection of a small number of LPS molecules into coagulation of blood into a semi-solid mass.^{10, 11} While the LAL test is remarkably sensitive and can detect extraordinarily low concentrations of LPS in samples, it suffers from a high frequency of false positives as well as high sensitivity to environmental conditions including small changes in pH and temperature.¹² A number of groups, inspired by nature's methods of detecting LPS, have worked on developing sensors specific for LPS using electrochemistry^{1, 13} and fluorescence,^{14, 15} with promising results if not quite the extraordinary sensitivity of the LAL test.

More difficult than detection of LPS is the identification of LPS, which can be used in principle as a diagnostic tool to identify bacterial infections. Strain-specific identification of bacteria is clinically important: while most strains of *Escherichia coli* are harmless, pathogenic strains can cause gastroenteritis, urinary tract infections,

1
2
3 neonatal meningitis, and Gram-negative pneumonia.¹⁶ *Pseudomonas aeruginosa* is another common bacterium that
4 is often only dangerous in opportunistic infections, where it can cause pneumonia, septic shock, or infections of the
5 lungs, urinary tract, and kidneys.¹⁷ *Salmonella enterica* causes up to 1.3 billion cases of disease each year, with a
6 wide range of clinical challenges depending on the subspecies and serovar.⁵ Similarly, benign and pathogenic
7 variants exist for *Serratia maracens* and *Klebsiella pneumoniae*.^{18, 19} More rapid differentiation among bacterial
8 strains and species would be advantageous in a wide range of clinical applications.

9 This differentiation, as opposed to nonspecific detection, of LPS is significantly more technologically
10 challenging and thus is at an earlier stage of development. LPS is composed of three parts: the lipid A anchored in
11 the cell membrane, the core oligosaccharide attached to the lipid A, and the O-antigen, consisting of a glycan
12 polymer. Although this general structure of LPS is conserved, there is remarkable variability in each of the
13 components of LPS depending on species of bacteria. This variability in LPS provides a handle for identification of
14 bacteria based on the detection and identification of LPS in solution. A number of groups are currently working on
15 methods to identify bacteria based on LPS detection through a variety of strategies. One recent report used
16 functionalized liposomes as sensors to identify LPS, but this method requires multiple experiments and varying
17 parameters such as temperature and the concentrations of SDS and EDTA to identify a single sample.²⁰

18 In contrast, a recently reported technique using surface plasmon resonance (SPR) to measure binding of
19 LPS to a small array of surface-immobilized antimicrobial peptides (AMPs) allows the discrimination among
20 different LPS samples without changing experimental conditions.²¹ AMPs have broad activity against a wide
21 variety of bacteria, befitting the fundamental role they play in the innate immune systems of most organisms.
22 Despite this broad activity, AMPs do not possess uniform activity, nor do they exhibit uniform binding to LPS.
23 These differences in the binding of AMPs to LPS are what permit the identification of LPS samples by recognition
24 of a particular pattern of binding. Seeking to broaden the scope of this strategy, we became interested in the
25 possibility of modifying the surface presentation of AMPs in order to study LPS discrimination. A number of
26 studies have shown that surface-immobilized AMPs can have remarkably different properties depending on
27 immobilization site, including both structure and activity.²²⁻²⁵ These studies have primarily examined cationic α -
28 helical AMPs, despite the remarkable breadth of AMP chemical and structural diversity. A straightforward increase
29 in complexity leads us to the sheep myeloid antimicrobial peptide SMAP-29, with a helix-turn-helix motif that
30 allows for additional three-dimensional presentations of the peptide when immobilized to a surface. This work
31 examines the differential presentation of the antimicrobial peptide SMAP-29 on a surface, how that presentation
32 affects binding to LPS, and how that binding to LPS leads to its ability to identify samples from a variety of
33 bacterial species and strains.

34 Experimental

35
36 **Materials.** Antimicrobial peptides were purchased from New England Peptide (Gardner, MA) and were of
37 minimum 85% purity. Thiols for self-assembled monolayers (**1**: 3,6,9-Trioxa-19-mercapto-nonadecan-1-ol and **2**:
38 1-amino-3,6,9,12,15,18-hexaoxonacosane-29-thiol, structures shown in Figure S1) were purchased from
39 ProChimia Surfaces (Sopot, Poland). Lipopolysaccharide samples were obtained from Sigma-Aldrich and List
40 Biological Laboratories as lyophilized powders purified via phenol extraction. Custom gold surfaces used in the
41 Biacore – borosilicate glass substrates were coated with a 5 nm layer of titanium then a 50 nm layer of gold
42 – were purchased from LGA Thin Films (Santa Clara, CA), while gold surfaces for the SPR Imager were purchased
43 from GWC Technologies (Madison, WI).

44 **Surface Preparation.** Immediately prior to use, the gold surfaces were cleaned with 5 minutes sonication in
45 methanol, dried with a stream of ultra-high purity nitrogen, then subjected to 15 minutes of ozonolysis in a UV-
46 ozone generator (Novascan PSD Series), followed by rinsing with deionized water and drying with UHP nitrogen.
47 Self-assembled monolayers (SAMs) of poly(ethylene glycol)-containing alkanethiols were assembled on the gold
48 surfaces to confer resistance to nonspecific adsorption of biomolecules. Thiols **1** and **2** (with functionalizable amine
49 terminus) were used in a 1:1 to 4:1 ratio. SAMs were formed by layering 300 μ L of a 0.2 mM total thiol solution in
50 70% ethanol / 30% water for one hour, washed with water then ethanol, then dried with UHP N₂.

51 **Peptide Immobilization – Biacore.** Each channel was independently functionalized by coupling of the thiol-
52 reactive N- γ -maleimidobutyl-oxysulfosuccinimide ester (sulfo-GMBS, Thermo Fisher) linker by flowing a freshly
53 prepared 25 mM solution of sulfo-GMBS in 100 mM phosphate pH 8.5 at 20 μ L/min for 5 minutes. Freshly diluted
54 peptides (45 μ M in pH 6.5 buffer with 5 mM TCEP) were attached via thiol-maleimide coupling by flowing at 20
55 μ L/min for 5 minutes. Any unfunctionalized maleimide groups were capped by flowing 50 mM mercaptoethanol at
56 30 μ L/min for 3 minutes. This procedure resulted in ~1000 RU of immobilized peptide.

Peptide Immobilization – SPR Imager. After washing with water and ethanol, and drying with UHP N₂, the sulfo-GMBS linker was attached by immersion in a 30 mM solution in a pH 8.5 phosphate buffer for 30 minutes.

Antimicrobial peptide solutions (5 μM in phosphate buffer at pH 6.5) were incubated with the reducing agent tris(2-carboxylethyl)phosphine hydrochloride (TCEP) for a minimum of 30 minutes and were then "printed" onto the functionalized gold surface using a continuous flow microspotter (Wasatch Microfluidics, Salt Lake City, UT) with two separate 30-minute flow cycles²⁶. Any remaining unfunctionalized sites were capped with 50 mM mercaptoethanol solution for 3 minutes.

SPR Experiments. SPR experiments were performed on either a Biacore T100 instrument or SPRImagerII (GWC Technologies, Madison, WI). One peptide was immobilized per channel or spot, respectively, while one out of every four channels or spots was functionalized only with mercaptoethanol to serve as a reference channel. For both instruments, fresh LPS samples at 10 μg/mL in phosphate buffer pH 7.4 were prepared for each experiment by dilution from a frozen 1 mg/mL stock in milliQ water. LPS samples were flowed at 20 μL/min for 5 minutes, followed by 5 minutes of running buffer at the sample flow rate. The LPS was removed from the surface by regeneration with a 50 mM NaOH solution in 30% acetonitrile. Each surface was pre-treated with at least 3 buffer and regeneration cycles prior to any LPS binding experiments.

Data Analysis. Loss of peptide activity over time was corrected by exponential or linear functions using repetitive injections of the same LPS sample (generally *E. coli* K235) over the course of the experiment as described previously.²¹ Time-corrected, reference-subtracted LPS binding was analyzed using R (R Foundation for Statistical Computing, Vienna, Austria). Linear discriminant analysis (LDA) was used to classify the LPS samples based on binding to the panel of AMPs. LDA generates classification functions that maximize inter-group variance while minimizing intra-group variance. Canonical scores for the top two classification functions are plotted to visualize the data clustering. The reported success rates for subgroups of peptides shown below are generated using the leave-one-out jackknife method, in which classification functions are generated without one data point, and the functions are used to classify that one data point. Alternatively, a training data set of LPS samples was used to develop LDA functions to classify the samples, which were then challenged with a separate test data set not used for the LDA functions. Each experiment was performed at least twice on independent, freshly prepared surfaces.

Table 1. Peptides Used in this Study

Peptide	Sequence	Charge at pH 7	Origin
SMAP-29 C-term	RGLRRLGRKI AHGVKKYGPT VLRIIRIAGC	9	Sheep
SMAP-29 N-term	CRGLRRLGRKI AHGVKKYGPT VLRIIRIAG	9	Sheep
SMAP-29 V14C	RGLRRLGRKI AHGCKKYGPT VLRIIRIAG	9	Sheep
SMAP-29 Y17C (hinge)	RGLRRLGRKI AHGVKKCGPT VLRIIRIAG	9	Sheep
SMAP-29 R5C (binding face)	RGLRCLGRKI AHGVKKYGPT VLRIIRIAG	8	Sheep
NA-CATHc	KRFKFFFKKL KNSVKKRAKK FFKKPKVIGV TFPFC	15	Snake ^{27, 28}
CPF-C1c	GFGSLLGKAL RLGANVLC	2	Frog ²⁹
Ac-cCP1	Ac-CSWLSKTAKK LENSARKKRIS EGIATAIQGG PR	4	Pig ³⁰
PL_1c	GWGSFFKKAH HVC	2	Fish ^{31, 32}
PLc	GWGSFFKKAH HVGKHVGGAA LTHYLC	4	Fish ³¹
CP1c	SWLSKTAKKL ENSAKKRIS EGIATAIQGGPR GGGC	5	Pig ³⁰

Supplemental Information. More complete details are included in the supplemental information, including the LPS samples used and more detailed procedures for surface preparation, SPR experiments, and data analysis.

Results and Discussion

The sheep myeloid antimicrobial peptide SMAP-29 is an attractive peptide for examining the impact of three-dimensional presentation on a surface: it has an interesting helix-turn-helix motif when in hydrophobic environments like that found when bound to LPS, it has high activity against a broad range of Gram-negative

bacteria, and it has previously been validated in LPS detection. Each helix independently has some antimicrobial activity, but significantly less than that of the full peptide.³³ SMAP-29 thus should have a range of binding affinities for LPS depending on the presentation of the peptide on the surface. Five versions of SMAP-29 were designed to test this hypothesis (Figure 1B). The C-terminal cysteine and N-terminal cysteine variants were expected to display on the surface in an upside-down “V” orientation. Two variants were made with cysteine mutations in the hinge region: V14C and Y17, to present the SMAP-29 peptide in a “V” formation. Lastly, R5C was included as a variant to block binding to the first helix, as the binding face of this helix would be facing the surface. Although we hypothesize that the different variants retain the same three-dimensional structure, we cannot rule out the possibility that the differently-immobilized SMAP-29 variants adopt different three-dimensional structures, as has previously been observed for α -helical peptides.³⁴

These peptides were immobilized on a custom Biacore gold surface with maleimide-functionalized self-assembled monolayers (SAMs) (Figure 1A) and were found to bind LPS at noticeably different levels. Several attempts to quantify the relative ability of each SMAP variant to discriminate LPS samples were hampered by a lack of a sufficient number of independent channels. Surprisingly, the different SMAP-29 peptides had different and unpredictable binding to different LPS samples. For example, the hinge-immobilized Y17C variant had higher binding the LPS from *E. coli* K235 than either the R5C or the N-terminal cysteine variants, but lower binding to LPS from *E. coli* O55:B5 (Figure 2A). Similarly, the R5C analog, which would be expected to exhibit reduced binding to LPS by blocking the binding face of the N-terminal helix, did indeed show lower binding to *E. coli* K235 and O128:B12 than the other two variants, but had increased binding to LPS from *E. coli* O55:B5 compared to the Y17C version.

This unpredictable binding to LPS samples from different strains of *E. coli* suggested the possibility of distinct binding modes, allowing us to use a panel of SMAP-29 peptides to discriminate among LPS samples. Indeed, a panel of three SMAP-29 variants and no other AMPs on a single chip (along with a reference channel) were quite sufficient to reliably identify a panel of LPS from four *E. coli* and one *P. Aeruginosa* strains (Figure 2B). For this analysis, the N-term, R5C, and Y17C variants were chosen, corresponding to an “upside down” presentation, a one-helix blocking presentation, and a hinge-immobilized presentation. A leave-one out jackknife calculation where the discrimination functions were calculated leaving out one data point, and then classifying the remaining data point, correctly classified the left out data point in 100% of cases.

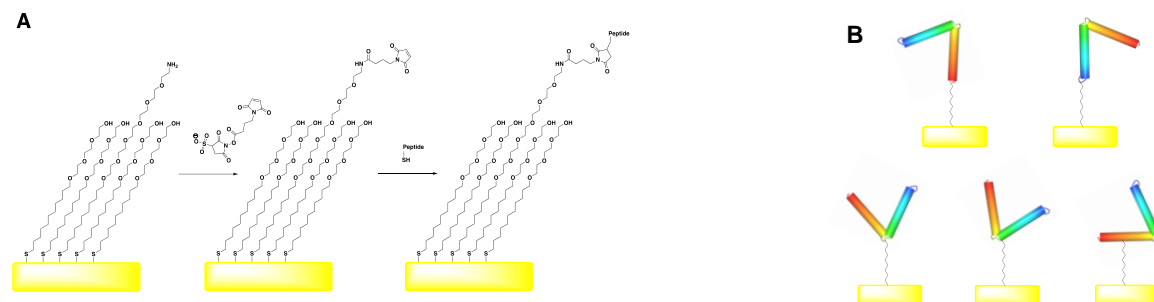
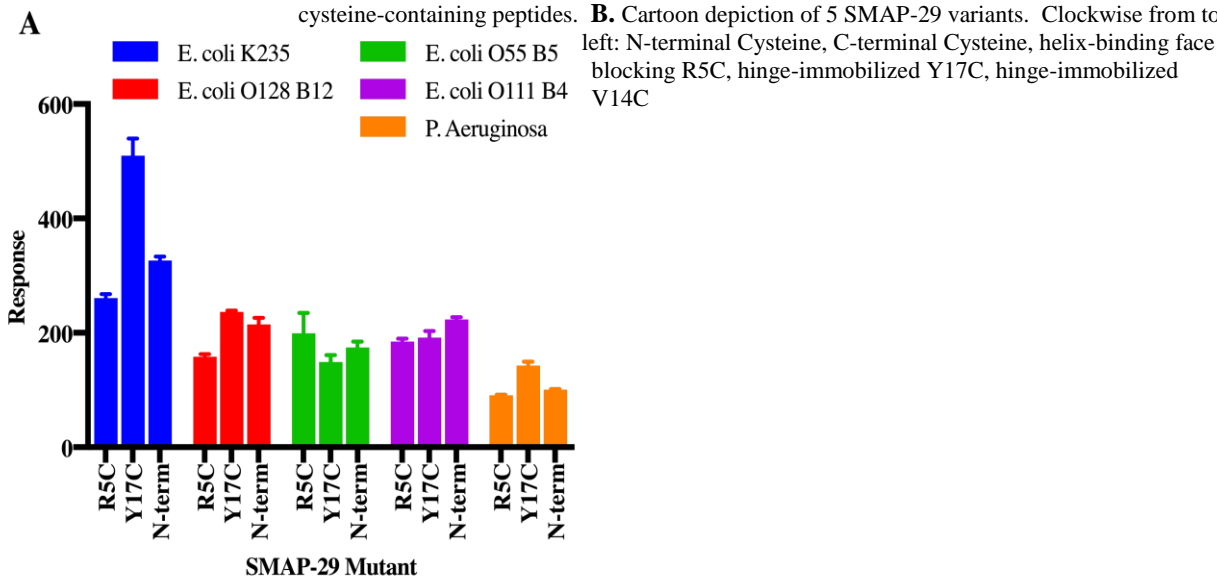


Figure 1. A. Schematic of self-assembled monolayers on gold with bioresistant poly(ethylene glycol) moiety. Amine-terminated thiols are functionalized with sulfo-GMBS at pH 8.5 to yield a maleimide functionality, which is used as a tether for cysteine-containing peptides. B. Cartoon depiction of 5 SMAP-29 variants. Clockwise from top



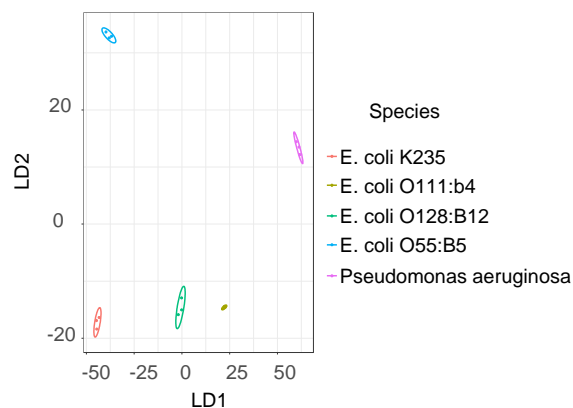


Figure 2. A. LPS binding profiles for 3 SMAP-29 variants on a Biacore T100. **B.** Linear discriminant analysis of a panel of 1 *P. Aeruginosa* and 4 *E. coli* strains using the panel of 3 SMAP-29 variants shown in part A..

To expand the range of analytes distinguishable by this method, we switched from a 4-channel Biacore T100 to an SPR Imaging system capable of analyzing a larger panel of peptides on a single chip. Preparation of the surface remained the same as that described in the experiments performed on the Biacore system, until the peptide immobilization step. At that point, peptide solutions were prepared in a 96-well plate, and a continuous flow microspotter (CFM) was used to expose 48 separate regions of the gold surface to individual solutions corresponding to a single well from the 96-well plate. This could be repeated to functionalize up to 96 individual regions of the surface. Up to twelve peptides were used, with one spot of every column of four left blank to use as a reference. The remaining procedure, including LPS solution flow and surface regeneration conditions, was the same as for the Biacore.

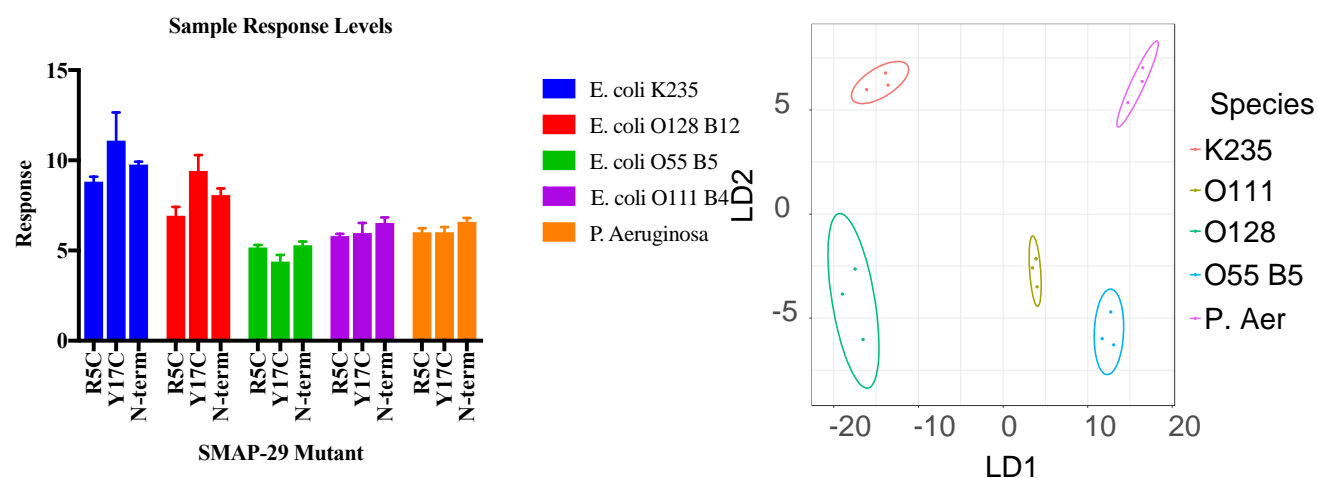


Figure 3. A. Binding profiles for three SMAP-29 variants with LPS from four *E. coli* strains and *P. Aeruginosa*. Both the absolute level of LPS absorbed and the relative propensity to bind different LPS samples differ for the SMAP-29 variants. **B.** Representative linear discriminant analysis of a panel of 1 *P. Aeruginosa* and 4 *E. coli* strains using a panel of 3 SMAP-29 variants using an SPRImager. This particular analysis is a repeat of that shown in Figure 2 using a Biacore T100 and uses SMAP-29 N-term, R5C, and Y17C, a subset for which the full data set is shown in Figure S2.

As with the Biacore, using the SPRImager showed noticeable distinct binding levels of LPS to different SMAP-29 peptides (Figure 3A). The LDA using the SMAP-29 N-term, R5C, and Y17C variants as shown in Figure 3 is repeated using the SPRImager (Figure 3B). Although the discrimination functions generated were different, the analysis clearly shows the capability of this panel to discriminate among LPS samples.

Use of the SPRImager allowed simultaneous analysis of all five SMAP-29 variants, along with a panel of seven additional AMPs. The additional AMPs included have a range of lengths, charges, and origins, and are listed in Table 1. This larger array permits the use of all five SMAP-29 variants to discriminate LPS samples. This larger panel is able to generate discrimination functions for a larger panel of 11 LPS samples from five different bacterial species, with a jackknife success rate of 97% (Figures 4, S3). Use of the SPRImager also permitted direct comparison of the ability of different SMAP-29 variants on the same gold surface to discriminate among a panel of LPS samples, avoiding the possible variability of preparing antimicrobial peptides immobilized to SAMs on different gold surfaces. Figure 5 shows the results of a LDA using only 1 peptide to try to discriminate among the 11 LPS variants. Several of the SMAP-29 variants were among the better discriminators of LPS, but there was clear variation within the SMAP-29 variants as well as the other AMPs examined. Of particular note is that the discrimination ability of a particular AMP is unrelated to its binding affinity to LPS (Figure 6).

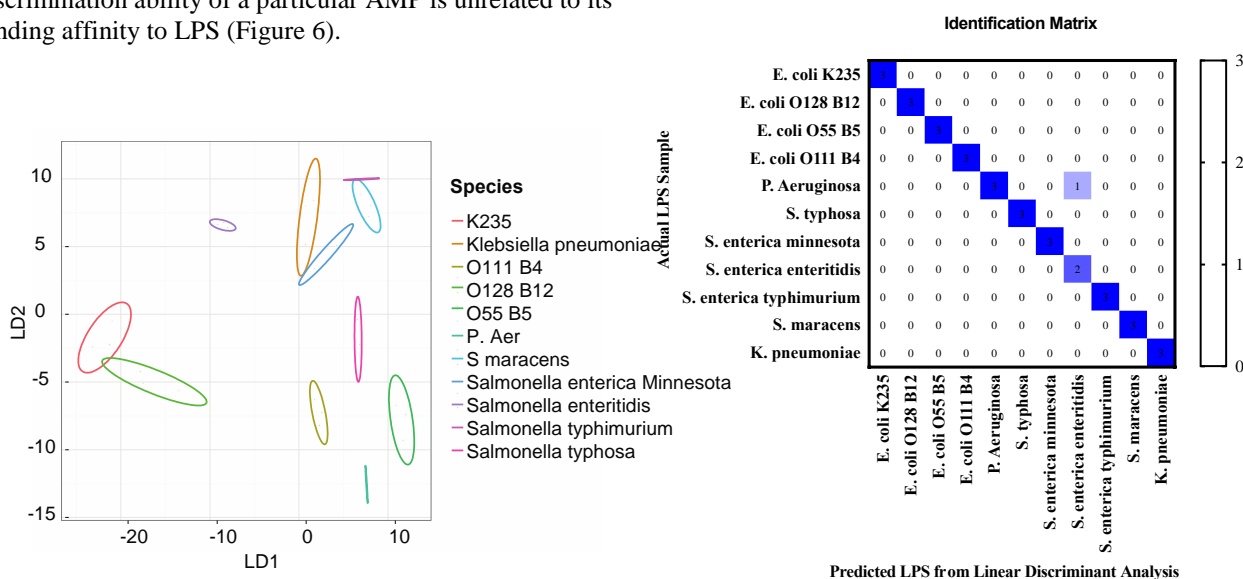


Figure 4. A. Linear discriminant analysis of a panel of 11 LPS samples from four different bacterial species using a panel of 5 SMAP-29 variants using an SPRImager. **B.** A jackknife analysis showed that the LDA functions generated from this data correctly identified 97% of samples (32/33).

It was straightforward to reproducibly identify the single AMP best able to discriminate among LPS samples (Figure 5). It was significantly more challenging and less reliable to predict whether adding an additional peptide would result in a higher identification rate, or which peptide would most improve discrimination. Pairwise comparisons (Figure S4) and a variety of three-peptide comparison strategies (Figures S5 and S6) fail to show clear trends. Neither binding affinity, nor the range of binding affinities, nor single-peptide identification rate, nor structural similarity or difference was reliably predictive in identifying the “best” panel of AMPs. However, this difficulty in identifying the “best” variant of SMAP-29 for LPS discrimination and identification results from the same root causes that allow the different SMAP-29 variants to be used for LPS discrimination.

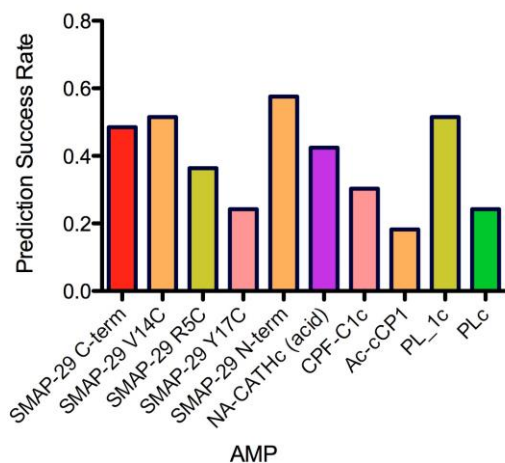


Figure 5: Single AMP Prediction Success. LDA was performed as described above, but was limited to one AMP at a time. Thus the prediction rate of 0.48 for the C-terminally immobilized SMAP-29 corresponds to correctly identifying 48% of the samples. Note that the SMAP-29 variants range from 24% (Y17C) to 58% (N-term).

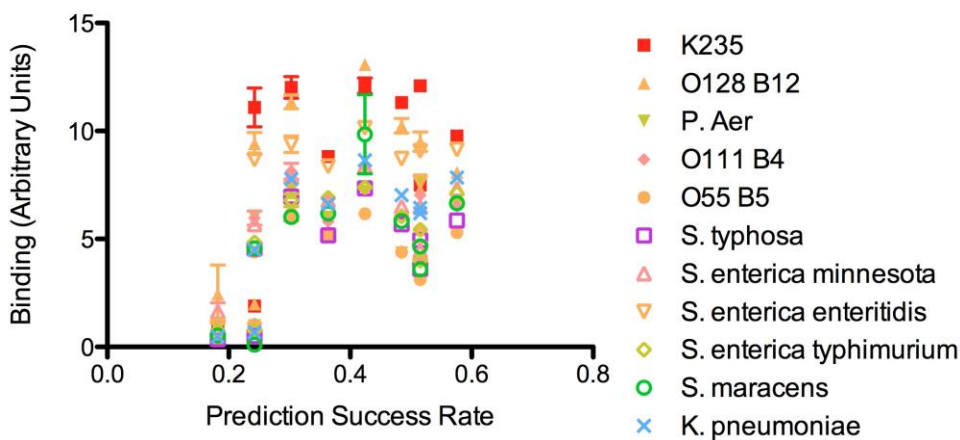


Figure 6. The magnitude of LPS bound to an AMP-decorated surface does not correlate with the ability of an AMP to distinguish between different LPS samples. Each column represents a different AMP, although the labels are not shown for clarity.

Indeed, the increased discriminatory power of the panel of SMAP-29 variant allowed us to extend this analysis to a larger, more diverse panel of 13 LPS samples from six different bacterial species. Again using only the 5 SMAP-29 variants, a training data set of three data points per AMP-LPS interaction was used to develop LDA functions, which were then challenged with a separate set of four data points per LPS sample. The success rate in identification of the training set was 100% (39/39 correctly identified samples), and the test data set correct identification rate was 86% (45/52 samples). The identification success for the training set is shown in Figure 7A, and the LDA scores for each sample are shown in Figures 7B and S8. Four of the seven misidentifications still correctly identified the bacterial species, simply misidentifying the specific strain, leading to a correct species identification rate of 94%. The corresponding LDA canonical score plots for the training set and the identification matrix for the test data set are shown in Figures S6 and S7, respectively. A two-dimensional plot showing the canonical scores for the different LDA functions is not as clear for this sample, as the first, second, and third orthogonal functions each contain significant discriminatory power. This is illustrated showing the canonical scores from each combination of LD1, LD2, and LD3 in Figures S9-S11.

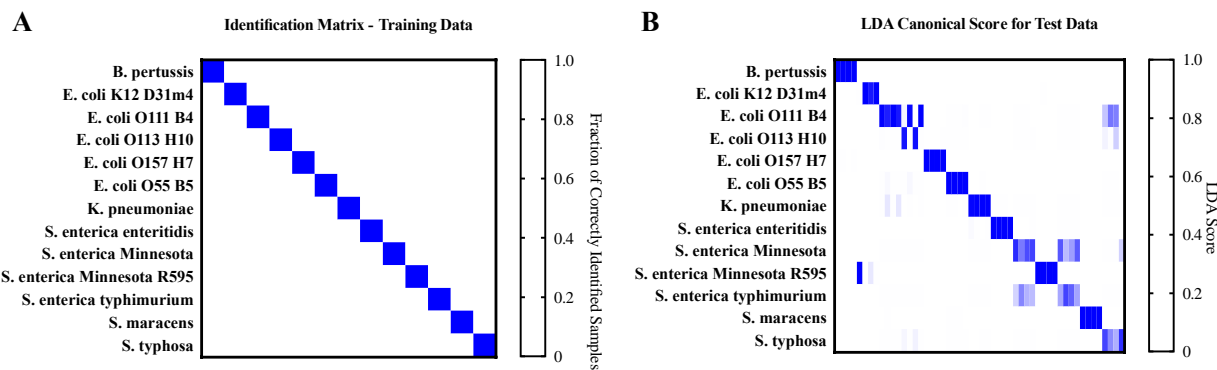


Figure 7. Expanded data set using all five SMAP-29 variants, with 3 data points for each LPS sample in the training set (A), and four data points for each LPS sample in the test set (B). This sample correctly identified 45 of 52 samples, for a success rate of 86.5%.

Conclusions

SMAP-29 was chosen as a model system to investigate how the three-dimensional presentation of AMPs on a surface influences binding to LPS, and whether those binding differences can be used to optimize discrimination of LPS from different bacterial strains. The helix-turn-helix motif found in SMAP-29 is more complicated than previously examined linear α -helical AMPs, and provides additional possibilities for the three-dimensional presentation of the AMP presented to the solution as binding sites for the LPS. Indeed, by simply changing the immobilization site for a given peptide, the resulting change in how the peptide is presented modulates binding. The resulting binding specificity of the different presentations permits a small array of SMAP-29 peptides to discriminate among a panel of LPS samples. It is unknown whether the marked change in binding modes that enables the discrimination accuracy of different SMAP-29 variants is a general feature or a characteristic unique to SMAP-29.

An unforeseen finding of this work is that the different immobilization variants of a given peptide resulted in sufficiently distinct LPS binding profiles to allow the use of *only* variants of a single peptide to discriminate among a panel of LPS samples. Each additional SMAP-29 variant added to the analysis resulted in a higher accuracy in LPS determination. Additionally, an analysis using all five SMAP-29 variants was more accurate than an analysis using any five of the seven non-SMAP-29 AMPs examined. This was not simply due to high binding levels; high binding levels were not predictive of discrimination accuracy.

It is difficult to precisely identify the cause of the high discrimination power of each SMAP-29 variant studied. The differential binding could be due to a simple differential presentation (right-side up versus upside down versus one binding face facing the surface) as originally designed. However, given that previous reports have shown that even simple short α -helical peptides can adopt very different three-dimensional structures depending on which terminus is conjugated to a surface,³⁴ we cannot rule out the possibility that the different immobilization sites result in different three-dimensional structures, either in solution or when bound to LPS.

This high discrimination power of the panel of SMAP-29 variants—regardless of the cause—allowed us to expand the power of LPS identification. Using an array of only 5 SMAP-29 variants and a small training set of just three binding measurements per LPS sample, we were able to correctly identify the LPS in a test set of 13 different LPS samples from six different clinically important bacterial species at a high success rate. This high success rate includes correctly identifying whether strains of *E. coli* were pathogenic (O157:H7, O111:B4, O55:B5) or nonpathogenic (O113:H10, K12), and even includes moderate success at identifying substrains of *Salmonella enterica*. The high discriminatory power of an array of AMP variants leads directly to the high success rates in difficult identification tests of LPS from clinically relevant non-pathogenic and pathogenic bacteria.

Conflicts of Interest

There are no conflicts to declare.

Acknowledgments

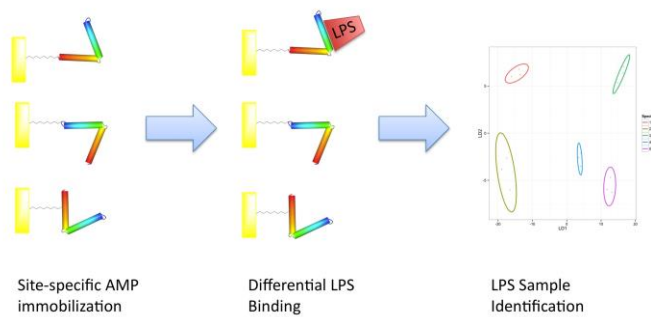
This research was performed while TMR held an NRC-CBD Research Associateship at the Combat Capabilities Development Command Soldier Center (formerly the US Army Natick Soldier Research, Development, and Engineering Center).

References

1. M. S. Mannoor, S. Zhang, A. J. Link and M. C. McAlpine, *Proceedings of the National Academy of Sciences*, 2010, **107**, 19207-19212.
2. F. B. Mayr, S. Yende and D. C. Angus, *Virulence*, 2014, **5**, 4-11.
3. C. J. Paoli, M. A. Reynolds, M. Sinha, M. Gitlin and E. Crouser, *Crit Care Med*, 2018, **46**, 1889-1897.
4. C. Blackwell, S. Moscovis, S. Hall, C. Burns and R. J. Scott, *Front Immunol*, 2015, **6**, 44-44.
5. B. Coburn, G. A. Grassl and B. B. Finlay, *Immunol Cell Biol*, 2006, **85**, 112-118.
6. A. Hass, M. I. Rossberg, H. L. Hodes, A. C. Hyatt and D. S. Hodes, *J Pediatr*, 1986, **109**, 265-269.
7. Y. Nakagawa, T. Murai, C. Hasegawa, M. Hirata, T. Tsuchiya, T. Yagami and Y. Haishima, *Journal of Biomedical Materials Research Part B: Applied Biomaterials*, 2003, **66B**, 347-355.
8. E. C. Hort and W. J. Penfold, *Journal of Hygiene*, 1912, **12**, 361-390.
9. T. Hartung and A. Wendel, *Altex*, 1995, **12**, 70-75.
10. F. B. Bang, *Bull Johns Hopkins Hosp*, 1956, **98**, 325-351.
11. J. Levin, P. A. Tomasulo and R. S. Oser, *J Lab Clin Med*, 1970, **75**, 903-911.
12. P. F. Rolansky and T. J. Novitsky, *J Clin Microbiol*, 1991, **29**, 2477-2483.
13. Z. She, K. Topping, M. H. Shamsi, N. Wang, N. W. C. Chan and H.-B. Kraatz, *Analytical Chemistry*, 2015, **87**, 4218-4224.
14. S. K. Lim, P. Chen, F. L. Lee, S. Mochhala and B. Liedberg, *Analytical Chemistry*, 2015, **87**, 9408-9412.
15. S. h. Voss, R. Fischer, G. n. Jung, K.-H. Wiesmüller and R. Brock, *Journal of the American Chemical Society*, 2007, **129**, 554-561.
16. J. P. Nataro and J. B. Kaper, *Clinical Microbiology Reviews*, 1998, **11**, 142-201.
17. K. Mathee, G. Narasimhan, C. Valdes, X. Qiu, J. M. Matewish, M. Koehrsen, A. Rokas, C. N. Yandava, R. Engels, E. Zeng, R. Olavarietta, M. Doud, R. S. Smith, P. Montgomery, J. R. White, P. A. Godfrey, C. Kodira, B. Birren, J. E. Galagan and S. Lory, *Proceedings of the National Academy of Sciences*, 2008, **105**, 3100-3105.
18. V. L. Yu, *New England Journal of Medicine*, 1979, **300**, 887-893.
19. R. Podschun and U. Ullmann, *Clinical Microbiology Reviews*, 1998, **11**, 589-603.
20. M. Rangin and A. Basu, *Journal of the American Chemical Society*, 2004, **126**, 5038-5039.
21. J. R. Uzarski and C. M. Mello, *Analytical Chemistry*, 2012, 7359-7366.
22. S. H. North and C. R. Taitt, *Langmuir*, 2015, **31**, 10791-10798.
23. S. H. North, J. Wojciechowski, V. Chu and C. R. Taitt, *Journal of Peptide Science*, 2012, **18**, 366-372.
24. Y. Li, S. Wei, J. Wu, J. Jasensky, C. Xi, H. Li, Y. Xu, Q. Wang, E. N. G. Marsh, C. L. Brooks and Z. Chen, *The Journal of Physical Chemistry C*, 2015, **119**, 7146-7155.
25. L. Shen, N. W. Ulrich, C. M. Mello and Z. Chen, *Chemical Physics Letters*, 2015, **619**, 247-255.
26. S. Natarajan, A. Hatch, D. G. Myszka and B. K. Gale, *Analytical Chemistry*, 2008, **80**, 8561-8567.
27. H. Zhao, T.-X. Gan, X.-D. Liu, Y. Jin, W.-H. Lee, J.-H. Shen and Y. Zhang, *Peptides*, 2008, **29**, 1685-1691.
28. F. A. de Latour, L. S. Amer, E. A. Papanastasiou, B. M. Bishop and M. L. van Hoek, *Biochem Biophys Res Commun*, 2010, **396**, 825-830.
29. J. M. Conlon, M. Mechkarska, E. Ahmed, J. Leprince, H. Vaudry, J. D. King and K. Takada, *Comp Biochem Physiol C Toxicol Pharmacol*, 2011, **153**, 350-354.
30. J. Y. Lee, A. Boman, C. X. Sun, M. Andersson, H. Jornvall, V. Mutt and H. G. Boman, *Proc Natl Acad Sci U S A*, 1989, **86**, 9159-9162.
31. A. M. Cole, P. Weis and G. Diamond, *J Biol Chem*, 1997, **272**, 12008-12013.
32. J. Cho, H. Choi and D. G. Lee, *J Microbiol Biotechnol*, 2012, **22**, 1367-1374.
33. B. F. Tack, M. V. Sawai, W. R. Kearney, A. D. Robertson, M. A. Sherman, W. Wang, T. Hong, L. M. Boo, H. Wu, A. J. Waring and R. I. Lehrer, *European Journal of Biochemistry*, 2002, **269**, 1181-1189.

- 1
2
3 34. Z. Wang, X. Han, N. He, Z. Chen and C. L. Brooks, *The Journal of Physical Chemistry B*, 2014, **118**,
4 5670-5680.
5
6
7
8
9
10
11

12 Table of Contents Entry:
13



26 Site-specific immobilization of an antimicrobial peptide permits sensing and identification of lipopolysaccharide
27 samples from a range of Gram-negative bacteria.
28
29
30
31
32
33
34
35
36
37
38
39
40
41
42
43
44
45
46
47
48
49
50
51
52
53
54
55
56
57
58
59
60